Polymer Journal

REGULAR ARTICLE

Morphology Development in Asymmetric Poly(styrene-*b*-*tert*-butylacrylate) Thin Films by Solvent Annealing

By Melvina LEOLUKMAN,[1] *Young-Hye* LA,[2] *Xuefa* LI,[3] *and Padma* GOPALAN[1,*]

Morphology dependence of asymmetric poly(styrene-*b*-*tert*-butylacrylate) [P(S-*b*-tBA)] thin film on casting solvent, annealing solvent and annealing time was investigated. Two casting solvents, toluene and propylene glycol monomethyl ester acetate (PGMEA), and two annealing solvents, *p*-xylene and *tert*-butylacrylate (tBA), were studied. The casting solvent dominated the initial morphology. P(S-*b*-tBA) film cast from toluene resulted in inverted phase (PtBA cylinders in PS matrix) and the one cast from PGMEA led to normal phase (PS cylinders in PtBA matrix) morphology. The annealing solvents preference to either the majority or the minority block in combination with the annealing time controlled the orientation of the cylinders. When the annealing solvent preferentially interacted with the majority block in the as-cast film, a metastable highly ordered perpendicular cylinder morphology was trapped. The best conditions to obtain perpendicular PS cylinders were casting P(S-*b*-tBA) film from PGMEA and annealing in tBA vapor for 20 and 25 min on silicon and NaCl substrates respectively.

KEY WORDS: Solvent Annealing / Block Copolymer / Polystyrene / Poly(*tert*-butylacrylate) /

The ability of block copolymers (BCPs) to self-assemble into highly ordered spherical, cylindrical, or lamellar domains in the sub 50 nm length scale[1–4] combined with suitable functionality in a selected block (sensitivity to ultraviolet, electron-beam, acid or base) has been exploited for nanopatterning applications.[5–8] For patterning a dense periodic array of lines or dots using either cylinder or lamella forming BCP thin film, it is crucial to control the orientation and registration of the BCP domains to the underlying substrate.

In thin film, the BCP interfaces (substrate-BCP and BCP-air) dictate the orientation of the microdomains.[9] Generally the polymer blocks have different interfacial energies, which result in preferential interaction with the substrate for one of the blocks and with air for the other block. These preferential interactions predominantly lead to parallel orientation of the domains.[10–12] In addition to the interfacial interactions, the thickness of the film also plays an important role in the final morphology.[9,12–14] Various methods have been used to control the microdomain orientation, such as tailoring interfacial interactions between BCP and substrate *via* random copolymer brushes,[15,16] controlling film thickness,[9,12–14] using chemically patterned substrate[17–19] and graphoepitaxy,[20,21] and applying external fields (for instance electric fields,[22] shear forces,[23] and temperature gradients[24]). For these methods to result in an equilibrium structure, thermal annealing in vacuum is required during the application of the external field or after coating the BCP on the modified substrate. However thermal annealing above the glass transition temperature of the two blocks for an extended period of time is not a viable option for thermally sensitive polymers.

Solvent assisted morphology development at room temperature is an attractive alternative to direct the orientation of temperature-sensitive BCP thin films, where highly directional field due to solvent evaporation and the increased mobility in the film owing to the presence of the solvent guide the structural rearrangement through the thickness of the film. The reports so far in the literature on solvent assisted morphology of asymmetric BCPs can be classified into two categories. In the first category, the orientation and ordering of BCP microdomains can be achieved during the deposition process by controlling "solvent evaporation" rate.[25–31] In the second category, the morphology of film cast from a good solvent for both blocks can be modified by "solvent annealing" in vapors with preferential interaction to one block.[32–37] From these studies it appears that the morphology obtained from solvent annealing process depends on (a) magnitude of solvent-polymer interaction, (b) solvent vapor pressure, (c) annealing time, and (d) film thickness. Although the morphology obtained through solvent annealing is often a metastable morphology, if the glass transition temperatures of the blocks are well above room temperature the structure obtained has long-term "stability" to be utilized as a template.

It is often hard to predict the conditions required for solvent annealing to trap non-equilibrium structures. Therefore, each BCP system needs to be examined for a variety of solvents and annealing times. One such system which is interesting for nanopatterning and as a photo-resist material is poly(styrene-*b*-*tert*-butylacrylate) [P(S-*b*-tBA)].[38] However the tBA block is

[1]Department of Materials Science and Engineering, University of Wisconsin-Madison, Madison, Wisconsin 53706, USA
[2]Department of Chemical and Biological Engineering, University of Wisconsin-Madison, Madison, Wisconsin 53706, USA
[3]Advanced Photon Source, Argonne National Laboratory, Argonne, IL 60439, USA
*To whom correspondence should be addressed (Tel: +1-608-265-4258; Fax: +1-608-262-8353, E-mail: pgopalan@wisc.edu).

susceptible to degradation in the presence of acid or heat.[31,39] Hence thermal annealing is not a viable option to facilitate self-assembly of P(S-*b*-tBA) system. Here we utilized solvent annealing to control the self-assembly of P(S-*b*-tBA) thin film into vertically oriented cylindrical domains. We report studies on morphology development of asymmetric P(S-*b*-tBA) thin film as a function of casting solvent, annealing solvent, and annealing time, as well as summarize the optimum conditions to obtain perpendicular cylinders. We also report the first use of a monomer (tBA) and a common photoresist solvent [propylene glycol mono methyl ester acetate (PGMEA)] as annealing and casting solvent respectively for controlling the BCP morphology and orientation in thin film.

EXPERIMENTAL

Asymmetric P(S-*b*-tBA) with molecular weight (M_n) of 108.3 kg mol^{-1}, polydispersity of 1.14 and PS weight fraction of 0.30 was purchased from Polymer Source, Inc. P(S-*b*-tBA) films were prepared by spin casting a solution of 1 wt % P(S-*b*-tBA) in toluene or PGMEA onto a freshly cleaved NaCl or silicon substrate at 3000 rpm for 1 min. Thickness measurement by Rudolph Auto EL null Ellipsometer of the cast films from PGMEA and toluene on silicon substrate showed a film thickness of 22 nm and 38 nm respectively. The resulting films were dried above the solvent boiling point for 1 min before annealing in tBA or *p*-xylene vapor to pre-determined times. The annealed P(S-*b*-tBA) films were dried immediately and picked up by a Transmission Electron Microscope (TEM) grid after dissolving the NaCl substrate in distilled water. The films were stained by RuO_4 vapor before viewing with bright field LEO 912 TEM at 120 kV accelerating voltage. The mass contrasts between the PS block, which was selectively stained by RuO_4, and the unstained PtBA block resulted in darker image of PS block in the bright field TEM. The film morphology on silicon substrate was evaluated by LEO 1530 Field Emission Scanning Electron Microscopy (SEM) and Grazing Incidence Small Angle X-ray Scattering (GISAXS) techniques. The SEM electron beam is known to damage PtBA domain making it appear dark in the SEM images.

RESULT AND DISCUSSION

Thermal annealing of P(S-*b*-tBA) film at 160 °C for two days in vacuum results in deprotection of *t*-butyl group into acrylic acid and subsequent condensation of poly(acrylic acid) to poly(acrylic anhydride), which changes the effective volume fraction of the blocks and therefore the resulting morphology.[40] Hence, solvent annealing was investigated to mitigate this problem. We mainly examined two casting solvents, toluene and PGMEA; and two annealing solvents, namely tBA and *p*-xylene. PGMEA is a common solvent for many photoresists; however its role as a casting solvent on BCP morphologies, potentially of interest for BCP lithography, has not been evaluated in the literature so far. Likewise the compatibility of a monomer such as tBA with its polymer (PtBA) is likely to be high due to their similar chemical structures. Hence, tBA constitutes a good solvent for PtBA blocks. However, the use of monomers as annealing solvent is also not reported so far in the literature. Here we investigate the morphology dependence of P(S-*b*-tBA) on annealing time, annealing solvent and casting solvent. Unless otherwise mentioned, the samples were cast on NaCl substrates and the morphologies were examined by TEM.

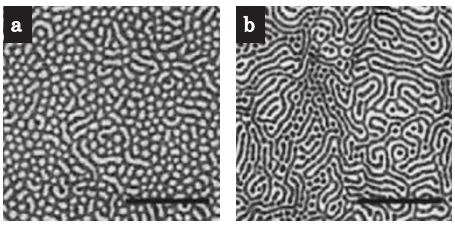

Figure 1. TEM images of P(S-*b*-tBA) as-cast from (a) toluene showing inverted morphology and (b) PGMEA showing normal morphology. The scale bar is 500 nm.

From the BCP composition (0.30 weight fraction of PS block), we expect the PS block to form cylinders in the PtBA matrix. However, films as-cast from toluene showed inverted phase consisting of a mixture of parallel (∥) and perpendicular (⊥) PtBA cylinders (Figure 1a: In the TEM images, PS appeared dark due to staining and PtBA appeared bright). The inverted phase is attributed to the preferential swelling of the PS block by toluene making the solvent-swelled PS block the majority block. As the thickness of the film is less than the d-spacing, it is highly unlikely that the observed morphology is a perforated lamella morphology. The second casting solvent that we examined was PGMEA, which preferentially interacts with the PtBA block due to its polar nature. This preferential interaction resulted in normal phase morphology, which consisted of a mixture of ∥ and ⊥ PS cylinders in the as-cast film (Figure 1b). Since films cast from both PGMEA and toluene showed mixed morphology, we explored the solvent annealing conditions to achieve exclusively either ⊥ or ∥ cylinders, which is of interest for BCP lithography.

Studies on Films Cast from PGMEA and Annealed in tBA

We studied the effectiveness of tBA, which is a monomer of PtBA with a relatively low boiling point of 61–63 °C, as an annealing solvent. Films were cast from PGMEA on both NaCl and silicon substrates and the development of morphology while annealing with tBA was observed by TEM (Figure 2) and SEM (Figure 3). In films cast from PGMEA on NaCl substrate the as-cast normal phase consisting of a mixture of ∥ and ⊥ PS cylinders was preserved through the first 22 min annealing in tBA vapor (Figure 2b and 2c). On further increasing the annealing time to 25 min, the enhanced mobility in the film led to the formation of large $5 \times 5\,\mu m^2$ hexagonally packed ⊥ PS cylinder regions (Figure 2d). Transition to a mixture of ∥ and ⊥ PS cylinders was observed when the film was annealed for 30 min (Figure 2e). Further annealing to 40 min led to ∥ PS cylinders (Figure 2f). Annealing beyond 43 min resulted in delamination of the film from the substrate. When cast from PGMEA on silicon substrate and annealed for

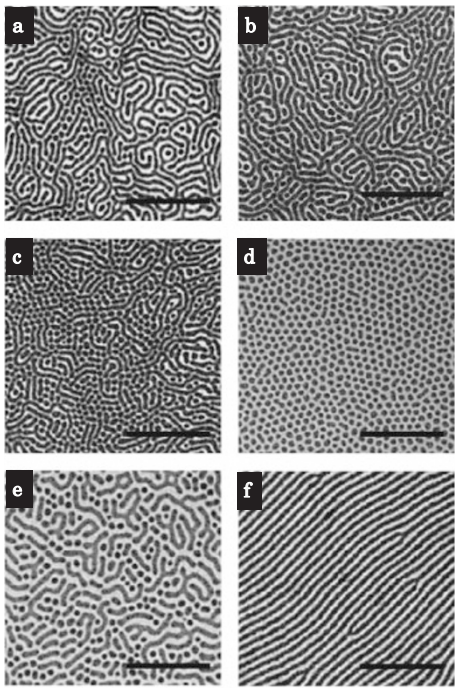

Figure 2. TEM images of P(S-*b*-tBA) cast from PGMEA and annealed in tBA vapor for 0 (a), 10 (b), 22 (c), 25 (d), 30 (e), and 40 (f) min. The scale bar is 500 nm.

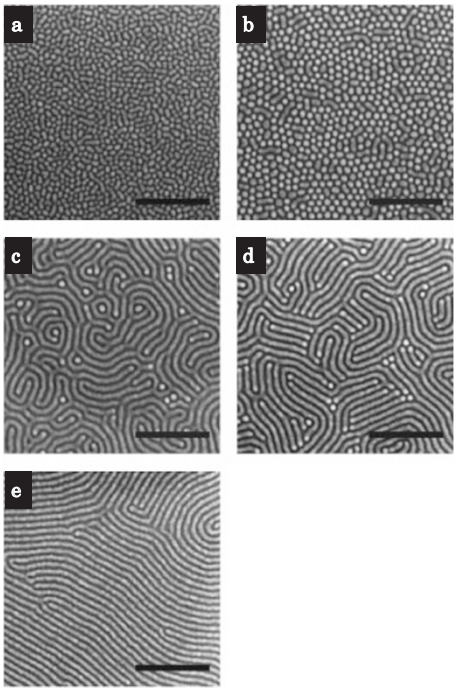

Figure 3. SEM images of P(S-*b*-tBA) cast from PGMEA on silicon wafer and annealed in tBA vapor for 10 (a), 20 (b), 25 (c), 30 (d), and 43 (e) min. In SEM images, PS appears bright and PtBA appears dark. The scale bar is 500 nm.

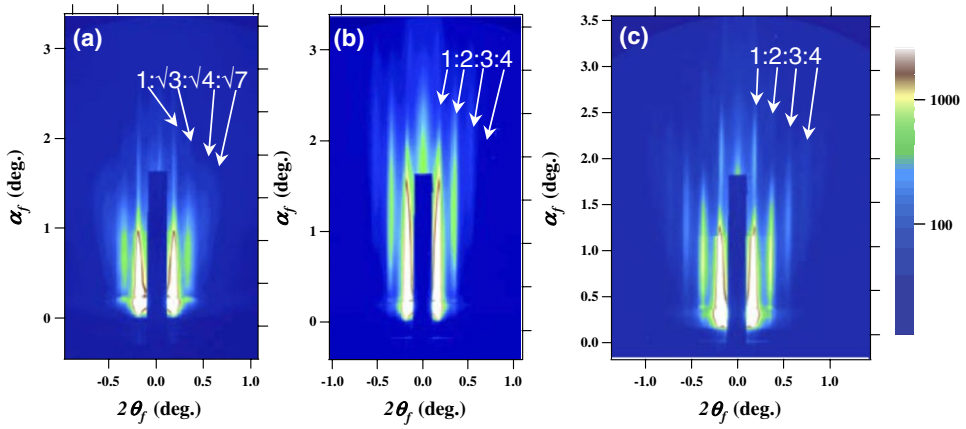

Figure 4. A 2D GISAXS image of scattered intensity I(2θ, α_f), where 2θ and α_f denote the in-plane and out-of-plane scattering angles. The incidence angle was 0.18 degree. GISAXS image of P(S-*b*-tBA) cast from PGMEA on silicon wafer and annealed in tBA vapor for (a) 20 min, where four scattering peaks with ratio of 1:$\sqrt{3}$:$\sqrt{4}$:$\sqrt{7}$ can be seen from each side of the beam stop indicating that the PS dots were hexagonally arrayed; and (b) 25 min and (c) 30 min, where four scattering peaks with ratio of 1:2:3:4 were observed.

10 min in tBA vapor, a normal phase consisting of a mixture of disordered ∥ and ⊥ PS cylinders was observed (Figure 3a). Increasing the annealing time to 20 min resulted in ordered ⊥ PS cylinders with d-spacing of 52.3 ± 3.2 nm by image analysis (Figure 3b). Increasing the annealing time to 25 min led to transition from ⊥ to ∥ PS cylinders (Figure 3c). Further annealing for 30 and 43 min resulted in larger regions of aligned ∥ PS cylinders (Figure 3d and 3e). Hence, irrespective of the substrate, *i.e.*, NaCl or silicon, similar trends were observed in the morphology development by solvent annealing (from mixed morphology to ⊥ PS cylinders to ∥ PS cylinders). The minor time difference between film cast on NaCl and silicon substrate can be attributed to possible differences in polarity of the substrates.

The observed morphologies of the films cast on silicon wafers were further confirmed by GISAXS. The 2D GISAXS image recorded on a MARCCD detector is a map of scattered intensity I(2θ, αf), where 2θ and αf denote the in-plane and out-of-plane scattering angles respectively (Figure 4). In the GISAXS image of the film annealed for 20 min in tBA, four scattering peaks that correspond to 1:$\sqrt{3}$:$\sqrt{4}$:$\sqrt{7}$ can be seen on each side of the beam stop (Figure 4a) confirming the

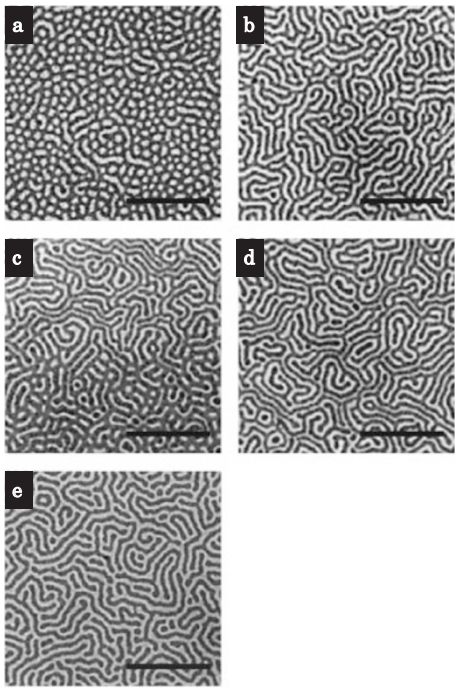

Figure 5. TEM images of P(S-*b*-tBA) cast from toluene and annealed in tBA vapor for 0 (a), 10 (b), 20 (c), 30 (d), and 40 (e) min. The scale bar is 500 nm.

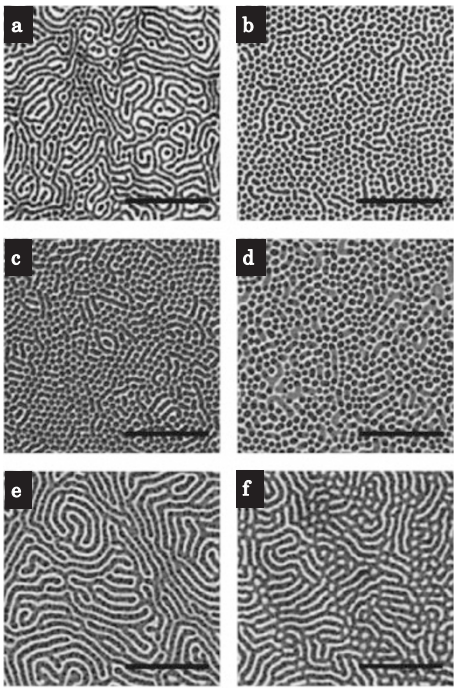

Figure 6. TEM images of P(S-*b*-tBA) cast from PGMEA and annealed in *p*-xylene vapor for 0 (a), 3 (b), 5 (c), 10 (d), 20 (e), and 30 (f) min. The scale bar is 500 nm.

hexagonal packing of the ⊥ PS cylinders. The cylinder d-spacing calculated from the Bragg's equation (d-spacing = $2\pi/q^*$ with q^* being the position of the primary diffraction peak) was 50.8 nm, which is consistent with the SEM result. To ensure X-ray penetration into the full depth of the film, the GISAXS measurements were done at incident angle (0.18°) that was greater than the polymer film critical angle (0.16°). Therefore the observed morphology is indeed cylinders standing up in a hexagonal pattern throughout the thin film. Increasing the annealing time to 25 min led to a distinct transition in the GISAXS image where 4th order scattering peaks with ratio 1:2:3:4 corresponding to lamellar morphology was observed (Figure 4b). As the film thickness is less than the d-spacing of the BCP, the morphology observed can be ⊥ lamella or one layer of ∥ cylinders, which would show similar GISAXS scattering pattern. In this case, the initial morphology was PS cylinders in PtBA matrix and the tBA vapor preferentially interacts with the PtBA matrix. Hence, it is unlikely that the BCP rearranges into lamellar morphology. Therefore, we infer that the GISAXS scattering peaks should correspond to ∥ PS cylinders in PtBA matrix. Further annealing to 30 min (Figure 4c) preserves the ∥ PS cylinders morphology with scattering peak ratios of 1:2:3:4.

Studies on Films Cast from Toluene and Annealed in tBA

The phase transitions in a toluene-cast P(S-*b*-tBA) thin film annealed in tBA vapor were studied as a function of annealing time. Annealing the film for 10 min in tBA vapor led to a change in morphology from a mixture of ∥ and ⊥ PtBA cylinders in PS matrix in the as-cast film (Figure 5a) to predominantly ∥ PtBA cylinders in PS matrix (bright stripes in a dark matrix) (Figure 5b). Longer annealing time of 30 min resulted in stripe morphology (Figure 5d). The preferential swelling of the PtBA block by the tBA vapor at longer annealing times of 40 min led to a distinct transition from the inverse phase, *i.e.*, ∥ PtBA cylinders in PS matrix (bright stripes in dark matrix) at 10 min annealing (Figure 5b) to the normal phase, *i.e.*, ∥ PS cylinders in PtBA matrix (dark stripes in bright matrix) (Figure 5e).

Studies on Films Cast from PGMEA and Annealed in *p*-Xylene

We also examined *p*-xylene as an annealing solvent as it preferentially interacts with the PS block. Films cast from PGMEA and annealed for 3–10 min in *p*-xylene vapor resulted in a transition from mixed ∥ and ⊥ PS cylinders to predominantly ⊥ PS cylinders morphology (Figure 6b, 6c and 6d). At longer annealing times, swelling of PS block by *p*-xylene is likely to increase PS effective volume fraction in the BCP making PtBA the minority block. Hence, inverted phase with PtBA stripes was observed after 20 min annealing (Figure 6e). Depending on the degree of swelling of the PS block, the stripes observed can be either ∥ PtBA cylinders or ⊥ lamellar morphology. At 30 min annealing a transition to a mixed inverted phase of PtBA stripes and dots was observed (Figure 6f). The presence of both dots and stripes led us to conclude that the observed morphology is a mixture of ∥ and ⊥ PtBA cylinders.

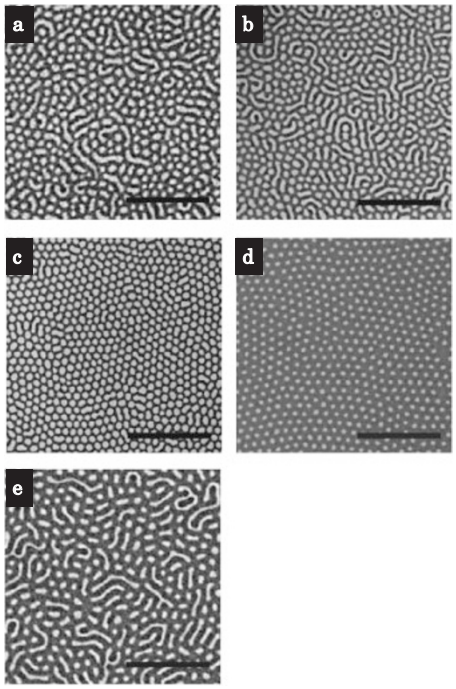

Figure 7. TEM images of P(S-*b*-tBA) cast from toluene and annealed in *p*-xylene vapor for 0 (a), 3 (b), 5 (c), 10 (d), and 20 (e) min. The scale bar is 500 nm.

Studies on Films Cast from Toluene and Annealed in *p*-Xylene

As discussed above, films cast from toluene showed inverted phase of PtBA cylinders in PS matrix (Figure 7a). At 3 min annealing in *p*-xylene vapor, the initial morphology of inverted phase consisting mixed parallel and perpendicular PtBA cylinders was preserved (Figure 7b). Annealing these films in *p*-xylene vapor will preferentially swell the PS block, which is the majority phase in the toluene-cast film. The effective plasticization of the PS matrix is likely to aid in the development of $\perp$ PtBA cylinders. Thus, further annealing to 5 and 10 min resulted in predominantly $\perp$ PtBA cylinders (Figure 7c and 7d). The decreasing cylinder diameter and the increasing spacing between cylinders from 5 to 10 min annealing may be attributed to the preferential interaction between PS and *p*-xylene that most likely drives PS to the film surface. As the observed structures are non-equilibrium inverse phase structures the domain size changes through the annealing process. When the film was annealed for 20 min, a mixture of $\parallel$ and $\perp$ PtBA cylinders was observed (Figure 7e). In the following section the observations on the effect of annealing time, casting solvent and annealing solvent on the morphology are summarized.

Effect of Annealing Time

The main factor that limits maximum annealing time is eventual delamination of the film. The P(S-*b*-tBA) films delaminate when annealed beyond 43 min. Within the annealing window (0–43 min), the as-cast morphology was developed by the annealing solvent based on its preference for one or the other blocks. It is well known that solvent vapor reduces the interfacial energy between polymer blocks and the surface/interface as well as increases the mobility in the film. In general, given sufficient time to undergo solvent-mediated structural rearrangement, parallel cylinders will result. For example in the PGMEA-cast, and 40 min tBA annealed film $\parallel$ PS cylinders was observed (Figure 2f). When cast from toluene and annealed in *p*-xylene for 30 min, a transition to more parallel PtBA cylinders was observed (Figure 7e). However, metastable states such as perpendicular cylinders can be trapped at shorter annealing times as seen in Figure 2d ($\perp$ PS cylinders), 6b ($\perp$ PS cylinders) and 7c ($\perp$ PtBA cylinders).

The Effect of Casting Solvent

During spin casting process the glass transition temperature of the blocks increases above room temperature as the solvent evaporates, which essentially freezes the solution morphology. The initial morphology of the spin cast P(S-*b*-tBA) film is primarily governed by two factors: (a) solvent vapor pressure and (b) nature and magnitude of interaction between the polymer blocks and the casting solvents. Non-polar toluene and polar PGMEA preferentially interacts/swells PS and PtBA blocks respectively which explain the observed normal and inverted phase morphologies when the P(S-*b*-tBA) was cast from PGMEA and toluene respectively. Earlier studies[34] on asymmetric BCP have shown that inverted phase was also observed if the annealing solvent is selective to the minority block. For P(S-*b*-tBA) system we did see inverted phase, particularly when using toluene as casting solvent and *p*-xylene as annealing solvent. It should also be noted that any good solvent will have some affinity for both blocks. Hence, solvent vapor pressure, *i.e.*, how fast a solvent evaporates, is crucial in the spin casting process and will have some influence on the morphology. Thus the observed normal and inverted phase morphology were also contributed by the low vapor pressure of PGMEA (3.7 mm Hg) and the relatively higher vapor pressure of toluene (22.0 mm Hg). Therefore, a combination of the solvent-polymer interaction and the evaporation rates of the casting solvents lead to unique starting morphologies, which were further developed by the solvent annealing process.

Effect of Annealing Solvent

Depending on the nature of the annealing solvent, preferential swelling of one of the blocks will occur. In general the polar nature of tBA leads to the swelling of PtBA block resulting in a normal phase (PS cylinders). Non-polar *p*-xylene on the other hand preferentially interacts with PS block resulting in an inverted phase (PtBA cylinders). The orientation of the cylinders, *i.e.*, $\perp$ or $\parallel$ is also governed by the preference of the annealing solvent to either the majority or the minority block. Generally, we find that if the annealing solvent preferentially interacts with the majority block in the as-cast film (PS in toluene-cast films and PtBA in PGMEA-cast films), we can trap a metastable highly ordered perpendicular cylinder morphology (PtBA cylinder in toluene-cast films, and PS cylinders in PGMEA-cast films) at shorter annealing times. For

example, in Figure 2d, a PGMEA-cast film with a mixed ∥ and ⊥ PS cylinder developed into a hexagonally packed ⊥ PS cylinder on annealing in tBA vapor, which preferentially interacts with the majority PtBA block. Similarly in Figure 7c, a transition from a mixed ∥ and ⊥ PtBA cylinder into a hexagonally packed ⊥ PtBA cylinder was observed in a toluene-cast film on annealing in *p*-xylene vapor, which preferentially interacts with the majority PS block. Preferential interaction of the majority block with the annealing solvent primarily allows sufficient mobility in the BCP film to bring about structural reorganization within the annealing window of 43 min. From these studies, it is also apparent that the time scale within which phase transitions were observed is much shorter when annealed in *p*-xylene (<10 min) compared with tBA (20–30 min).

CONCLUSIONS

The effect of casting solvent, annealing solvent and annealing time on the morphology of asymmetric P(S-*b*-tBA) thin film was investigated. We studied two casting solvents, namely toluene and a common photoresist solvent PGMEA, and two annealing solvents, such as a monomer (tBA) and *p*-xylene. Some of the main conclusions from this study are: (a) Casting solvent has a dominating effect on the initial BCP morphology, which is then further developed by annealing solvents. Non-polar toluene and polar PGMEA preferentially interacts/swells PS and PtBA blocks respectively. Hence, P(S-*b*-tBA) film cast from toluene led to inverted phase morphology (*i.e.*, mixed PtBA ∥ and ⊥ cylinders in a PS matrix), while P(S-*b*-tBA) film cast from PGMEA gave rise to normal phase morphology (*i.e.*, mixed PS ∥ and ⊥ cylinders in a PtBA matrix); (b) The orientation of the cylinders can be controlled by the preference of the annealing solvent to either majority or minority block in the as-cast film in combination with the annealing time. In general, if the annealing solvent preferentially interacts with the majority block in the as-cast film (PS in toluene-cast films and PtBA in PGMEA-cast films), a metastable highly ordered perpendicular cylinder morphology (PtBA cylinder in toluene-cast films, and PS cylinders in PGMEA-cast films) can be trapped; (c) The best conditions to obtain ⊥ PS cylinders is to cast P(S-*b*-tBA) film from PGMEA and anneal in tBA for 20 and 25 min on silicon and NaCl substrates respectively; (d) The maximum annealing time for these films is about 43 min beyond which delamination of the film occurs; (e) PGMEA which is a common photoresist solvent can be potentially used as a casting or annealing solvent for other BCP thin films used in BCP lithography; (f) The selectivity of the annealing solvent to one of the domains can be increased by exploring their monomers as potential annealing solvents. In this study tBA, a low boiling point (61–63 °C) monomer, was an effective annealing solvent for P(S-*b*-tBA) film to obtain ⊥ PS cylinders.

Acknowledgment. We would like to acknowledge useful discussions with Prof. Paul F. Nealey, and Dr. Insik In. This work was supported by the UW-NSF Nanoscale Science and Engineering Center (DMR-0425880) and the DMR-NSF-CAREER 0449688. We also acknowledge the use of Materials Science Center Facilities and Medical School Electron Microscope Facility at University of Wisconsin-Madison. Use of the Advanced Photon Source was supported by the U. S. DOE, Office of Science, Office of Basic Energy Sciences, under Contract No. DE-AC02-06CH11357.

Received: January 20, 2008
Accepted: May 17, 2008
Published: July 16, 2008

REFERENCES

1. F. S. Bates, *Science*, **251**, 898 (1991).
2. F. S. Bates and G. H. Fredrickson, *Annu. Rev. Phys. Chem.*, **41**, 525 (1990).
3. G. H. Fredrickson and F. S. Bates, *Annu. Rev. Mater. Sci.*, **26**, 501 (1996).
4. I. W. Hamley, "The Physics of Block Copolymers," Oxford University Press, Oxford, 1998.
5. J. Y. Cheng, C. A. Ross, V. Z. H. Chan, E. L. Thomas, R. G. H. Lammertink, and G. J. Vancso, *Adv. Mater.*, **13**, 1174 (2001).
6. W. A. Lopes and H. M. Jaeger, *Nature*, **414**, 735 (2001).
7. M. Park, C. Harrison, P. M. Chaikin, R. A. Register, and D. H. Adamson, *Science*, **276**, 1401 (1997).
8. T. Thurn-Albrecht, J. Schotter, C. A. Kastle, N. Emley, T. Shibauchi, L. Krusin-Elbaum, K. Guarini, C. T. Black, M. T. Tuominen, and T. P. Russell, *Science*, **290**, 2126 (2000).
9. M. J. Fasolka, P. Banerjee, A. M. Mayes, G. Pickett, and A. C. Balazs, *Macromolecules*, **33**, 5702 (2000).
10. S. H. Anastasiadis, T. P. Russell, S. K. Satija, and C. F. Majkrzak, *Phys. Rev. Lett.*, **62**, 1852 (1989).
11. G. Coulon, B. Collin, D. Ausserre, D. Chatenay, and T. P. Russell, *Journal De Physique*, **51**, 2801 (1990).
12. M. J. Fasolka and A. M. Mayes, *Annu. Rev. Mater. Res.*, **31**, 323 (2001).
13. A. Knoll, A. Horvat, K. S. Lyakhova, G. Krausch, G. J. A. Sevink, A. V. Zvelindovsky, and R. Magerle, *Phys. Rev. Lett.*, **89**, 035501 (2002).
14. M. A. Vandijk and R. Vandenborg, *Macromolecules*, **28**, 6773 (1995).
15. E. Huang, L. Rockford, T. P. Russell, and C. J. Hawker, *Nature*, **395**, 757 (1998).
16. P. Mansky, Y. Liu, E. Huang, T. P. Russell, and C. Hawker, *Science*, **275**, 1458 (1997).
17. S. O. Kim, H. H. Solak, M. P. Stoykovich, N. J. Ferrier, J. J. de Pablo, and P. F. Nealey, *Nature*, **424**, 411 (2003).
18. L. Rockford, Y. Liu, P. Mansky, T. P. Russell, M. Yoon, and S. G. J. Mochrie, *Phys. Rev. Lett.*, **82**, 2602 (1999).
19. L. Rockford, S. G. J. Mochrie, and T. P. Russell, *Macromolecules*, **34**, 1487 (2001).
20. J. Y. Cheng, C. A. Ross, E. L. Thomas, H. I. Smith, and G. J. Vancso, *Adv. Mater.*, **15**, 1599 (2003).
21. R. A. Segalman, H. Yokoyama, and E. J. Kramer, *Adv. Mater.*, **13**, 1152 (2001).
22. T. L. Morkved, M. Lu, A. M. Urbas, E. E. Ehrichs, H. M. Jaeger, P. Mansky, and T. P. Russell, *Science*, **273**, 931 (1996).
23. R. J. Albalak, M. S. Capel, and E. L. Thomas, *Polymer*, **39**, 1647 (1998).
24. J. Bodycomb, Y. Funaki, K. Kimishima, and T. Hashimoto, *Macromolecules*, **32**, 2075 (1999).
25. K. Fukunaga, H. Elbs, R. Magerle, and G. Krausch, *Macromolecules*, **33**, 947 (2000).

26. J. Hahm and S. J. Sibener, *Langmuir*, **16**, 4766 (2000).
27. G. Kim and M. Libera, *Macromolecules*, **31**, 2569 (1998).
28. G. Kim and M. Libera, *Macromolecules*, **31**, 2670 (1998).
29. S. H. Kim, M. J. Misner, T. Xu, M. Kimura, and T. P. Russell, *Adv. Mater.*, **16**, 226 (2004).
30. M. Kimura, M. J. Misner, T. Xu, S. H. Kim, and T. P. Russell, *Langmuir*, **19**, 9910 (2003).
31. Z. Q. Lin, D. H. Kim, X. D. Wu, L. Boosahda, D. Stone, L. LaRose, and T. P. Russell, *Adv. Mater.*, **14**, 1373 (2002).
32. H. Elbs, C. Drummer, V. Abetz, and G. Krausch, *Macromolecules*, **35**, 5570 (2002).
33. H. Y. Huang, Z. J. Hu, Y. Z. Chen, F. J. Zhang, Y. M. Gong, T. B. He, and C. Wu, *Macromolecules*, **37**, 6523 (2004).
34. H. Y. Huang, F. J. Zhang, Z. J. Hu, B. Y. Du, T. B. He, F. K. Lee, Y. J. Wang, and O. K. C. Tsui, *Macromolecules*, **36**, 4084 (2003).
35. J. Peng, Y. Xuan, H. F. Wang, Y. M. Yang, B. Y. Li, and Y. C. Han, *J. Chemical Phys.*, **120**, 11163 (2004).
36. Y. Xuan, J. Peng, L. Cui, H. F. Wang, B. Y. Li, and Y. C. Han, *Macromolecules*, **37**, 7301 (2004).
37. Q. Zhang, O. K. C. Tsui, B. Du, F. Zhang, T. Tang, and T. B. He, *Macromolecules*, **33**, 9561 (2000).
38. Y.-H. La, I. In, S.-M. Sang-Min Park, R. P. Meagley, M. Leolukman, P. Gopalan, and P. F. Nealey, *J. Vac. Sci. Technol., B*, **25**, 2508 (2007).
39. D. Y. Ryu, K. Shin, E. Drockenmuller, C. J. Hawker, and T. P. Russell, *Science*, **308**, 236 (2005).
40. Y. H. La, E. W. Edwards, S. M. Park, and P. F. Nealey, *Nano Lett.*, **5**, 1379 (2005).